(12)

ANNUAL REPORT

INTERFACE ENGINEERING IN OXIDE FIBER/OXIDE MATRIX COMPOSITES

Contract No. N0014-89-J1459

for the period
March 1, 1993 to February 28, 1994

Principal Investigator

K. K. Chawla

Department of Materials and Metallurgical Engineering
New Mexico Institute of Mining and Technology
Socorro, NM 87801

Submitted to
Dr. S. G. Fishman
Project Manager
Office of Naval Research
Arlington, VA 22217

CONTENTS

SUMMARY

We have shown in earlier work that significant improvements in the mechanical properties of the alumina + 15w/o zirconia (PRD-166) fiber/borosilicate glass matrix and mullite (Nextel 480 and 550) fiber/mullite matrix composites could be achieved using interface engineering approach. This approach involves a control of the microstructure, roughness of the interface, and the thermal expansion mismatch between the fiber and matrix in order to improve the strength and fracture toughness of the composite. We have made a qualitative comparison of the elemental distribution in the PRD-166/glass (N51A) composites, with and without an SnO_2 coating, on fibers using secondary ion mass spectrometry (SIMS). The results confirmed that tin dioxide serves as an effective barrier between this fiber and the silica-based glass. The tensile strength and toughness of the interface between SnO_2 and flat alumina substrate were obtained by a laser spallation technique. An average tensile strength value of 0.32 ± 0.03 GPa and a toughness of 1.5 mJ/m^2 were obtained for this interface. The surface roughness of three alumina-type fibers, PRD-166, Nextel 610, and Saphikon, was quantitatively characterized by atomic force microscopy (AFM). PRD-166 fiber had the highest roughness, Saphikon was the smoothest, while Nextel 610 showed an intermediate roughness. Coefficients of thermal expansion (CTEs) of PRD-166/glass composites, with and without SnO_2 coating, were measured as a function of fiber volume fraction. The results indicated that the fiber breakage during processing played a more significant role than the fiber misorientation in the effective thermal expansion coefficient of the composite.

Two oxide fiber/oxide matrix composite systems, alumina fiber (Nextel 610)/glass matrix and mullite type fibers (Nextel 480 and 550)/mullite matrix, with and without interface coating, were prepared. We are in the process of characterizing the interface strength of these composites by indentation technique.

LIST OF TABLES

LIST OF FIGURES

I. INTRODUCTION

Composite materials capable of maintaining excellent strength and fracture toughness are required for high temperature structural applications. Ceramics and glasses exhibit relatively high thermal stability combined with low density and chemical inertness as compared with metals and polymers. As is well known, ceramics and glasses are very brittle and fail in a catastrophic manner. Continuous fiber reinforcement is one way of overcoming this lack of toughness. The increase in toughness of fiber-reinforced ceramic matrix composites results because a number of energy-absorbing mechanisms, such as fiber/matrix debonding, crack deflection, and fiber pullout, can be made to operate in these materials [1]. We have shown in earlier work that significant improvements in the mechanical properties of the alumina + 15w/o zirconia (PRD-166) fiber/borosilicate glass matrix and mullite (Nextel 480 and 550) fiber/mullite matrix composites could be achieved using interface engineering approach [2, 3]. In this approach, the microstructure of the interface, the strength and fracture toughness of the interface, the roughness of the interface, and the thermal expansion mismatch between the components are the important factors to be considered.

In this annual report, we report the following work:

- Microstructrual characterization of PRD-166 fiber/glass composites with and without an SnO_2 interphase by SIMS.
- Tensile strength of the interface between SnO_2/alumina.
- Surface roughness of three alumina type fibers.
- Thermal expansion of PRD-166 fiber/glass composites.

Two oxide fiber/oxide matrix composite systems, alumina fibers (Nextel 610)/glass matrix and mullite type fibers (Nextel 480 and 550)/mullite matrix (with and without interface coating), were prepared. The interface strength of these composites is quantitatively being characterized using indentation technique. Microstructure characterization and mechanical testing of the Nextel 610/glass matrix composite are also under progress. These results will be included in the next report.

II. MATERIALS

Three kinds of continuous alumina fibers, PRD-166 (α-alumina + 15 w/o zirconia), Saphikon (single crystal α-alumina), and Nextel 610 (α-alumina), were incorporated in a borosilicate glass matrix. Nextel 480 and Nextel 550 fibers were used in a mullite matrix. Nextel 480 is a polycrystalline fiber with an essentially mullite composition. The as-received Nextel 550 is not crystalline mullite but a mixture of δ-alumina and amorphous silica with mullite composition, which can be transformed to mullite when heated above 1200 °C. Mullite powder synthesized via a diphasic gel route in our laboratory was used as matrix materials. Tin dioxide fiber coating was used for PRD-166 and Saphikon fibers, while BN and BN/SiC (double coating) were used for Nextel 480 and Nextel 550, respectively. In the double coating, the outer layer was SiC. Nextel 610, a relatively smooth fiber, is the new fiber used in this work. The nominal compositions and some properties of the materials used are summarized in Tables 1 and 2, respectively.

III. EXPERIMENTAL PROCEDURE

3.1 Microstructural characterization of PRD-166/glass composite by SIMS

A VG SIMSLAB equipped with an MM12-12 quadrupole was used. The primary beam was 25 kV Ga^+ beam in the microprobe rastered mode. The characterization was done by ion mapping, that is, the secondary ion images were obtained over the region of interest by stepping the beam digitally and recording the intensity of a certain isotope as a function of position. The secondary ion images were correlated with the ion-induced electron micrographs from the same areas. The specimens were mounted on stubs using silver paint, baked for 0.5 h at 100 °C, then coated with Au-Pd. During the course of the secondary ion mass spectrometry analysis, the primary beam eroded the Au-Pd coating over only the analyzed area, and the rest of the coating provided a good path for charge dissipation.

3.2 Tensile strength and toughness of interface between SnO_2 and alumina

Circular disks (2-4 mm in thickness) were cut from a 10 mm diameter rod in a slow speed diamond saw. Alumina rod, 99.5+% pure, with no porosity was obtained from Coors, Inc. The disks were polished with 1 μm diamond paste and cleaned ultrasonically in acetone. Tin dioxide coating was applied to one side of the samples by a chemical vapor deposition process [3, 4]. A 0.5 μm thick aluminum film was deposited onto the back side of the substrate disk in a vacuum evaporator. Measurements of the tensile strength of the interface were carried out using laser spallation technique. The details of this technique can be found in ref. [5]. A 2.5 ns long pulse from Nd:YAG laser is focused on a 3 mm diameter spot onto the 0.5 μm thick aluminum film that is sandwiched between the back surface of a substrate of 1 mm thickness and a 2 mm thick plate of constraining fused quartz transparent to the laser wavelength. Fused quartz was mechanically attached to the substrate. Absorption of the laser energy in the confined aluminum film leads to a sudden expansion of the aluminum film, which, due to the axial constraints of the assembly, leads to the generation of a compressive stress pulse directed toward the SnO_2 coating/alumina substrate interface. A part of the compressive pulse is transmitted into the coating as the compression pulse strikes the interface. It is the reflection of this compressive pulse into a tensile pulse from the free surface of the coating that leads to the removal of the coating, given a sufficiently high amplitude. When the stress pulse reflects from the free surface of the coating, the free surface experiences a transient velocity, proportional to the profile of the stress pulse striking the free surface. The peak interface stress at the threshold laser fluence gives the interface strength.

3.3 Measurement of surface roughness of the fibers

Fiber samples were mounted by means of a double stick tape on aluminum stubs for examination in an atomic force microscope (AFM). In an AFM, the probe tip in the form of a microcantilever is placed a few angstroms from the sample surface. The AFM microcantilever is deflected by the interatomic repulsion between atom on the tip and atoms on the sample surface. A laser beam is used to measure the

deflection of the tip. A very sharp tip, a few atom wide, is attached to a micro-cantilever arm. The probe tip is brought in contact with the sample and scanned across the sample surface in a raster pattern. The deflection of the cantilever is monitored and this signal is used in a feedback loop to obtain an image of the surface.

3.4 Measurement of thermal expansion of the composites

Thermal expansion measurements were made with an Orton dilatometer (model 1000D). The thermal expansion of the composites was recorded in the temperature range of 25 - 500 °C. The experimental expansion values were obtained by averaging out the thermal expansion data over the temperature range of 25 - 500 °C, in intervals of 20 °C.

IV. RESULTS AND DISCUSSION

4.1 Microstructure of the interface

The efficiency of SnO_2 as a barrier between alumina and glass was confirmed by SIMS. A mapping of $120Sn^+$ by SIMS of a region of the coated fiber composite as well as the ion-induced secondary electron image of the same region are shown in Fig.1 (a, b). Fairly uniform tin dioxide coating around fibers can be seen. The coating appears large where the fibers intersect the surface at an angle. It would appear that tin is confined to the coating region. An advantage of SIMS over other techniques is the ability to map light elements, such as sodium. Figure 2(a,b) shows mapping of $23Na^+$ in the coated and uncoated fiber composites. Note the diffusion of Na^+ into the fiber as well as concentration near the interface in the uncoated fiber case. Such a diffusion of sodium ions seems be absent in the case of the SnO_2-coated fiber. Boron is another light element that is difficult to map in an electron microscope. Mappings of $11B^+$ showed, see Fig. 3, that there was some diffusion of boron from the glass matrix into the uncoated fiber.

4.2 Tensile strength and toughness of the interface

Adhesion strength between SnO_2 coating and polycrystalline alumina substrate was measured by a modified laser spallation technique at the Dartmouth college. Figure 4(a) shows a typical photodiode voltage corresponding to the velocity of the Al_2O_3 free surface. Figure 4(b) is the stress pulse profile corresponding to the fringe record of Fig. 4(a). In all the experiments the failure was observed at the interface. An average tensile strength value of 0.32 ± 0.03 GPa was obtained for the SnO_2/alumina interface. The strength determined by the laser spallation experiment should be independent of the inelastic processes since the interface separation takes place at a strain rate of almost 10^6 s^{-1}. The tensile strength of the interface was related to the interface intrinsic toughness through a relation using the concept of universal bonding correlation [6]:

$$\sigma^2_{max} = E_o G_{ci} / e^2 h.$$

It should be emphasized that the concept of universal bonding correlation is used only define the shape of the interface stress-separation curve. In this expression, h is the unstressed separation distance between the planes joining at the interface and E_o is the initial one-dimensional tensile straining modulus of the interface layer. Plugging in the appropriate values, this expression yields a value of 1.5 mJ/m^2 for the interface toughness. This value is very low in comparison to the expected intrinsic toughness value for hard interface, which is of order of 1 J/m^2. Certainly the measured low value is due to the interface flaws. An estimate for the interface flaw size can be made using this equation by using G_{ci} = 1 Jm/m^2 and = 0.32 GPa. This process yields a flaw size of 0.4 μm. Considering the polycrystalline structure of alumina, it is likely that the flaws of this size remain at interface upon the deposition of the SnO_2 coating.

4.3 Surface roughness of three alumina-type fibers

Quantitative information on fiber surface roughness was obtained by means of atomic force microscopy (AFM). Figure 5 is a grey level top view image, showing the surface morphology of PRD-166 fiber. A relatively large grain size (0.5 μm) of this fiber surface generates a very rough surface. Figure 5 also shows an elongated depression or an axial striation on the fiber surface, the depth of which is between 700

- 800 nm. This kind of defect, which may result from the fiber processing procedure, can be a big source of the surface roughness. The line scan on the surface of PRD-166 fiber, shown in Fig. 6, gives the corresponding surface roughness profile of the fiber. The surface morphology of Nextel 610 fiber is shown in Fig. 7, a grey level top view image. Comparing Figs. 5 and 7, one notes the marked difference in the surface morphology of PRD-166 and Nextel 610, both polycrystalline fibers. The smaller grain size of Nextel 610 (about 0.08 μm), gives a smoother surface. Figure 8 gives a line scan of the Nextel 610 fiber. Note the relative smoothness of this profile, cf. Fig. 6. The surface roughness of these polycrystalline fibers appears to scale with the grain size. Single crystal alumina (Saphikon) fiber is showed an unusual feature, namely steps on the fiber surface. Figure 9 shows a line scan on the Saphikon surface. Note the smooth with a step perpendicular to the fiber axis. Such steps on the fiber surface can be sites of stress concentration, which can decrease the fiber tensile strength dramatically [7].

Results of the surface roughness characterization are summarized in Table 3. Figure 10 serves to define the parameters in Table 3. It can be seen from Table 3 that the PRD-166 fiber had the highest roughness, Saphikon was the smoothest, while Nextel 610 fiber shown an intermediate roughness. Using the coefficients of thermal expansion of the three fibers and a glass matrix material, the radial strain at the fiber/matrix interface due to thermal mismatch and the gripping induced by the fiber surface roughness can be computed. Table 4 lists the values of the A/r ratio for each fiber. The maximum sliding resistance should be taken into account for fiber pullout behavior, and thus, the value of R_{max}/r ratio would give us the worst case scenario. Among the three fibers, the PRD-166 fiber has the greatest value of this ratio, 0.027. The radial strain at the fiber/coating interface consists of two parts: one due to the thermal mismatch between the fiber and interface, which can be either tensile or compressive, and the other one comes from the roughness induced clamping, which is always in compression. Comparing the ratio of the thermal mismatch portion of the radial strain at the interface of alumina fiber/tin dioxide coating, to the roughness contribution for PRD-166, Table 4, we see that the compressive radial strain is an order of magnitude greater than the tensile thermal portion. That is, the combined

effect of the two in the case of the PRD-166 fiber/tin dioxide interface will be rather tight gripping or clamping in the radial direction. Now let us see this effect in the Nextel 610 fiber/tin dioxide interface. Although the two parts of the radial strain at the fiber/coating interface have the same order of magnitude, the net effect in this case will create a small compressive strain in the radial direction. In the Saphikon fiber/tin dioxide interface, unlike the cases of PRD-166 and Nextel 610 fibers, the contribution of mismatch of the thermal expansion coefficients to the radial strain can compensate for the compressive radial strain due to the surface roughness, and the net result is a tensile strain. The net radial strains at the fiber/tin dioxide interface, listed in the last row of Table 4, show that the compressive radial strain at PRD-166/tin dioxide interface is expected to be 20 times greater than that at the Nextel 610/tin dioxide interface, and only at Saphikon/tin dioxide interface is the net radial strain tensile in nature. This leads to an understanding of how the surface roughness affects the interfacial bonding between the fiber and matrix.

4.4 Thermal expansion of PRD-166/glass composite

Experimental coefficients of thermal expansion (CTE) of the uncoated and tin dioxide coated fiber composites in the longitudinal and transverse directions were compared with the predicted values from various models. The transverse CTE values for both the uncoated and coated fiber composites, appeared to fit Schapery's model [8] more closely than any of the other models. Also the CTEs for the tin dioxide coated fiber composites appear to be closer to the theoretically predicted values as compared to the uncoated fiber composites. This is probably due to the fact that all of the models used for obtaining the CTEs assume perfect bonding between the fiber and matrix, without any chemical interactions at the interface. The effect of any kind of chemical reaction which might alter the interface characteristics is not taken into account. In the case of the uncoated fiber system, the bonding between the fiber and matrix has a strong chemical component to it (because of the high reactivity between alumina and silicate) and any reaction product(s) formed will, in all likelihood, have a different CTE and also affect the bonding in these systems. This is probably the reason for the observed discrepancies between the theoretical and experimental

values. The experimental CTE in the longitudinal direction for the coated fiber composites shows that the deviation from the theoretical prediction of Schapery's model appears more at the higher fiber volume fraction than at lower one. The fiber misorientation and breakage induced during processing could be one of the main reasons for these deviations. It turns out that the fiber breakage played a more significant role than the fiber mosorientation because fiber breakage resulted in short fibers which have a lesser constraint on the matrix than long, continuous fibers.

V. CONCLUSIONS

We have shown that secondary ion mass spectrometry (SIMS) can be used to generate elemental distribution maps in alumina type fiber/glass matrix composites. Our SIMS study of PRD-166/glass and PRD-166/SnO_2/glass composites shows that tin dioxide serves as an effective barrier between the (alumina + zirconia) fiber and silica-based glass. The tensile strength and toughness of the interface between SnO_2 and alumina, as determined by a laser spallation technique, were 0.32 GPa and 1.5 mJ/m^2, respectively.

Fiber surface roughness is a very important parameter along with the thermal mismatch between the components. Quantitative information was obtained by AFM on the degree of fiber surface roughness. PRD-166 fiber had the highest roughness, Saphikon was the smoothest, while Nextel 610 showed an intermediate roughness.

The investigation of CTE of PRD-166/glass composites showed that effects of chemical reaction at the interface, fiber breakage and fiber misorientation which occur during fabrication and/or handling of these composites must be accounted for as they can affect the CTE of the composites quite significantly. In the present composite system, the fiber breakage played a more significant role than the fiber misorientation because fiber breakage resulted in short fibers which had a lesser constraint on the matrix expansion than long, continuous fibers.

VI. REFERENCES

1. K. K. Chawla, **Ceramic Matrix Composites**, Chapman & Hall, London, 1993.
2. K. K. Chawla, Final Report to ONR, Contact No. N0014-89-J1459, Feb. 29, 1992.
3. K. K. Chawla, Annual report to ONR, Contract No. N0014-89-J1459, Feb. 28, 1993.
4. M.H. Siadati and K.K. Chawla, **Mater. Characterization, 27** (1991) 19.
5. A. Pronin, V. Gupta, J. Yuan, K. K. Chawla, and R. U. Vaidya, **Script Meta. et Mat., 28** (1993) 1371-1376.
6. J.H. Rose, J.R. Smith, and J. Ferrante, **Phys. Rev. B, 28** (1984) 2963.
7. D.M. Marsh, in **Fracture of Solids**, D. C. Drucker & J. J. Gilman (eds.), Interscience Publishers, New York, 1962, pp.119-42.
8. R. A. Schapery, **J. Comp. Mater., 2** (1969) 311.

VII. PUBLICATIONS

The following publications and presentations resulted from the research performed under this contract.

1. J.-S. Ha and K.K. Chawla, "Effect of SiC/BN Double Coating on Fibre Pullout in Mullite Fibre/Mullite Matrix Composites," **J. Mater. Sci. Lett., 12** (1993) 84.

2. K.K. Chawla, M.K. Ferber, Z.R. Xu, and R. Venkatesh, "Interface Engineering in Alumina/Glass Composites," **Mater. Sci. & Eng., A162** (1993) 35.

3. A. Pronin, V. Gupta, J. Yuan, K.K. Chawla, and R.U. Vaidya, "Tensile Strength of Interface between SnO_2 Coating and Alumina Substrate," **Scripta Met. et Mater., 28** (1993) 1371.

4. M.E. Fine, R. Mitra, and K.K. Chawla, "Internal Stress and Work Adhesion," **Scripta Met. et Mater., 29** (1993) 221.

5. M.K. Ferber, A.A. Wereszczak, L. Riester, R.A. Lowden, and K.K. Chawla, "Evaluation of the Interfacial Mechanical Properties in Fiber Reinforced Ceramic Composites," **Ceramic Sci. & Eng. Proc., 7- 8** (1993) 168.

6. K.K. Chawla, A. Choudhury, R. Venkatesh, and J.R. Hellmann, "Microstructural Charachterization by Secondary Ion Mass Sectrometry of (Alumina+Zicronia) Fiber/Glass Composites with and without a Tin Dioxide Interphase," **Materials Characterization, 31** (1993) 167.

7. K.K. Chawla, Z.R. Xu, A. Hlinak, and Y.-W. Chang, "Surface Characterization of Three Alumina-Type Fibers by Atomic Force Microscopy," in Proc. Conf. on Adv. Composites, N.P. Bansal (ed.), Amer. Ceram. Soc., Westerville, Ohio, 1993.

8. Z.R. Xu, K.K. Chawla, andX. Li, "Effect of High Temperature exposure on the Tensile Strength of Nextel 610 Fiber," **Mater. Sci. & Eng., A171** (1993) 249.

9. J. S. Ha, K. K. Chawla, and R.E. Engdahl, "Effect of Processing and Fiber Coating on Fiber/Matrix Interactions in Mullite Fiber/Mullite Matrix Composites", **Mater. Sci. & Eng., A161** (1993) 303.

10. J.-S. Ha, K.K. Chawla, and R.E. Engdahl, "The Effect of Precursor Characteristics on the Crystallization and Densification of Diphasic Mullite Gels,", **Ceramics International, 19** (1993) 299.

11. K. K. Chawla, Z. R. Xu, R. Venkatesh, and J. S. Ha, "Interface Engineering in Some Oxide/Oxide Composites," **Proceedings of 9th International Confernce on Composite Materials**, Madrid, Spain, 1993, Vol II, pp.788-95.

12. A. Wolfenden, K.K. Chawla et al.,"The Relation of Dynamic Elastic Moduli, Mechanical Damping and Mass Density to the Microstructure of Some Glass Matrix Composites," **J.Materials Science**, in press.

13. R.U. Vaidya, R. Venkatesh, and K.K. Chawla, "Thermal Expansion of PRD-166 Fiber Reinforced Glass Matrix Composites," **Composites**, in press.

BOOKS

1. K.K. Chawla, **Ceramic Matrix Composites,** Chapman & Hall, London, 1993, pp. 423.

PRESENTATIONS

1. Z.R. Xu, K.K. Chawla, and X. Li, "Effect of high temperature exposure on the Tensile strength of Alumina Fiber Nextel 610 ,"Materials Week, TMS and ASM Intl., Pittsburgh, PA., Oct. 18-22, 1993.

2. A. Wolfenden, K.K. Chawla, J.E. Gill, V. Thomas, A.J. Giacomin, R.U. Vaidya and R. Venkatesh, "Dynamic Elastic Moduli and Damping in Glass Matrix Ceramics, Including Temperature Dependence," Adv. Materials Conference, Albuquerque, October 25- 26, 1993.

3. K.K. Chawla, Z.R. Xu, R. Mitra and M.E. Fine, "Thermal Expansion of TiC Particle Reinforced Aluminum Matrix XD^{TM} Composites," Adv. Materials Conference, Albuquerque, October 25- 26, 1993.

IX. AWARDS & RECOGNITIONS

1. Member, International Committee on Composite Materials (ICCM)

2. Eschbach Visiting Scholar, Northwestern University, Evanston, IL..

3. Visitor, NSF Institute for Mechanics and Materials, Univ. of Calif. at San Diego, La Jolla, CA.

X. EDUCATIONAL ACCOMPLISHMENTS

One of the important objectives of any research in the universities should be to train students to do high quality research. Research activity can and should be rightly considered an educational activity. Planning experiments, collecting and analyzing data, and finally presenting the results, oral and written, to the community at large form part of this activity. Students attend weekly meeting where they present, defend, and get feedback on their work. They are in daily contact with the P. I. to discuss their work and related problems.

The personnel involved in this research are listed below.

Postdoctoral Research Associate

1. Z. R. Xu

Graduate Students

1. J. Groves (M.S.)
2. R. Roybal (M.S.)

Undergraduate Students

1. P. Tenorio
2. A. Neuman
3. B. Furman

APPENDIX A: REPORT DISTRIBUTION

Addressees	Number of Copies
Scientific Officer Code : 1131N Steven G. Fishman Office of Naval Research 800 North Quincy Street Arlington, Virginia 22217-5000	3
Administrative Grants Officer Office of Naval Research Resident Representative N68583 Administrative Contracting Officer University of New Mexico, RM 204 Bandelier Hall West Albuquerque, New Mexico 87131-0001	1
Director, Naval Research Laboratory Attn : Code 2627 Washington, DC 20375	6
Defense Technical Information Center Building 5, Cameron Station Alexandria, Virginia 22314	12
Mr. W.D. Peterson New Mexico Tech Socorro, New Mexico 87801	1

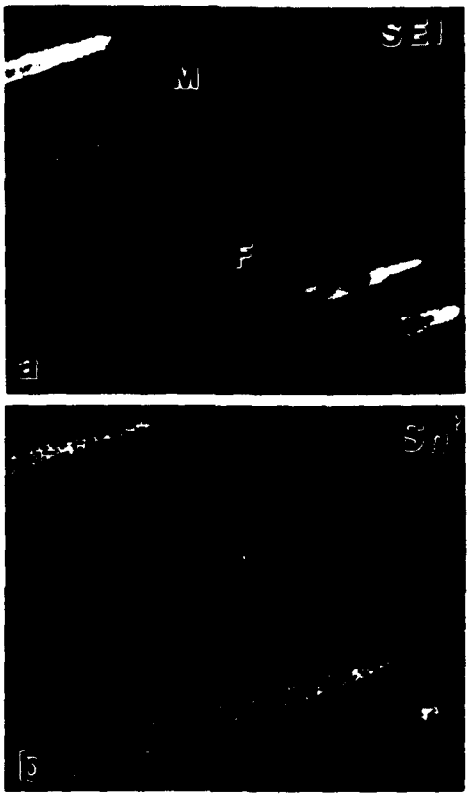

Fig. 1

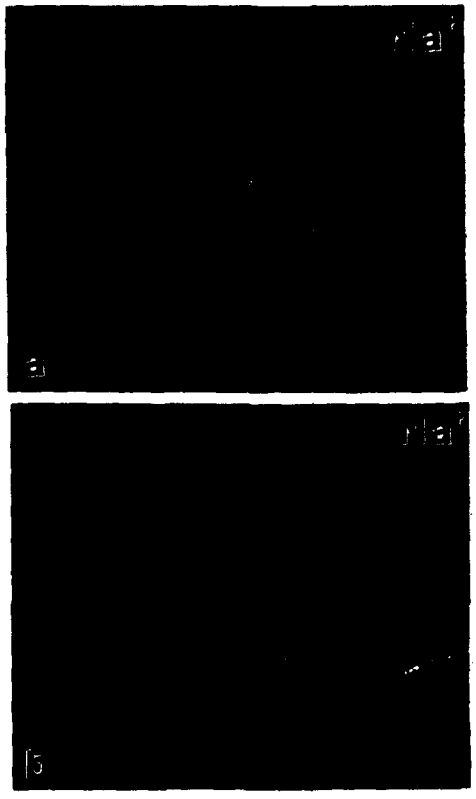

Fig. 2

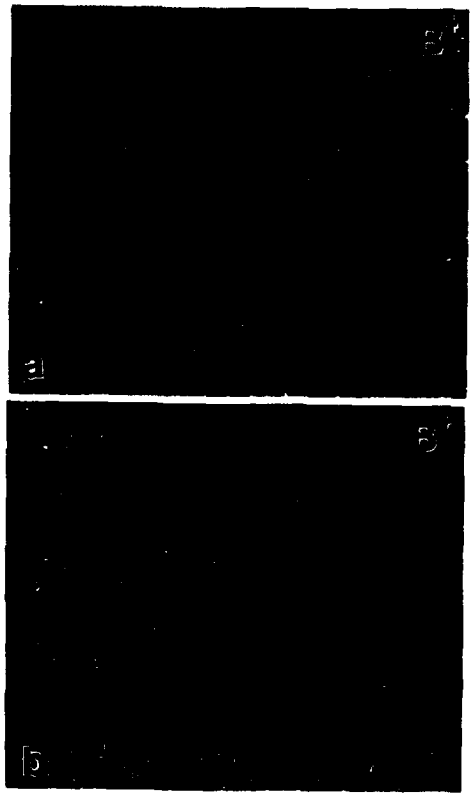

Fig. 3

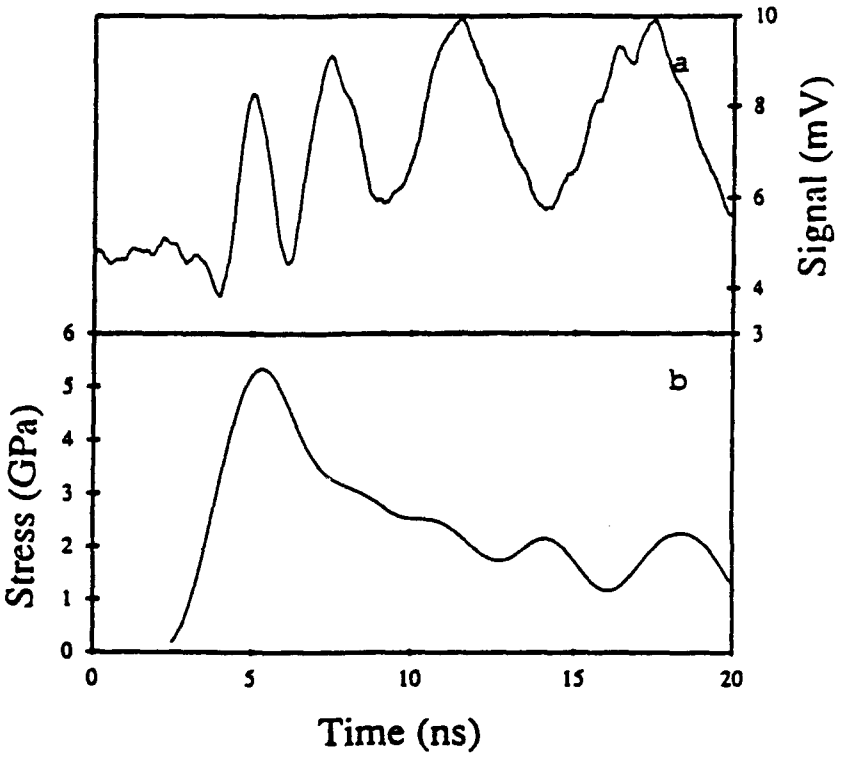

Fig.4

Fig. 5

Fig.6

Fig.7

Fig. 8

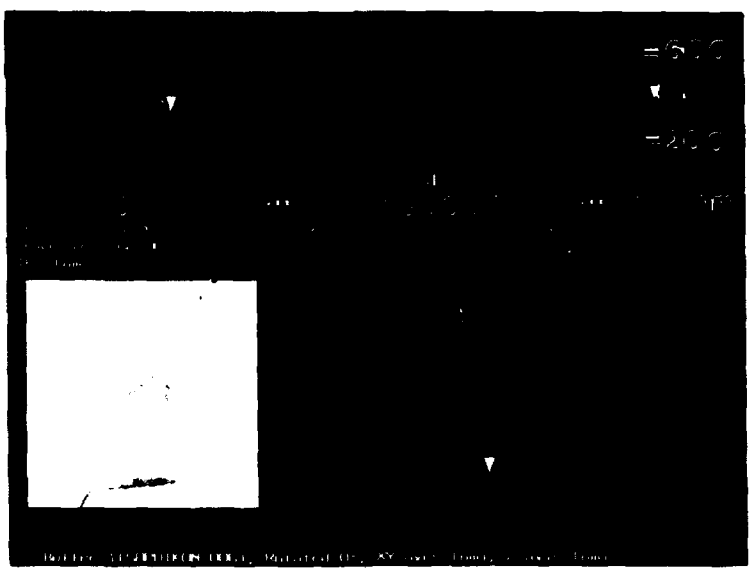

Fig. 9

$\mathbf{R_a}$ = Mean Roughness

$$\frac{1}{L}\int_0^L f(x)\,dx$$

where L = Length of Roughness Curve
f(x) = Roughness Curve

$\mathbf{R_{max}}$ = Maximum Roughness

Difference between the highest and lowest point

$\mathbf{R_z}$ = Ten–Point Average

Fig.10

Table 1. Composition and properties of fibers and fiber coatings

	PRD–166	Saphikon	Nextel 480	Nextel 550	Nextel 610	SnO_2	BN	SiC
Composition	ZrO_2: 15–20 Al_2O_3: 80–85	α–Al_2O_3	Al_2O_3: 70 SiO_2: 28 B_2O_3: 2	Al_2O_3: 73 SiO_2: 27	α–Al_2O_3	–	–	–
Melting point (°C)	1830	2053	1850	1850	2053	1630	3000	2220
Density (g/cm^3)	4.2	3.9	3.05	3.03	3.75	6.95	2.27	3.21
Tensile strength (MPa)	2070 (6.4)†	3150	1900 (51)†	2000 (51)†	1900	–	80–110	255–465#
Young's modulus (GPa)	380	380	220	193	373	233	60–80#	440–470#
CTE (10^{-6}/°C)	9	9.12 (∥ to c–axis) 7.95 (⊥ to c–axis)	4–5	4–5	9	5.23	5#	4.8#

Data of CVD materials
† Gauge length, mm

Table 2. Properties of matrices

	Melting point (°C)	Density (g/cm^3)	Temsile strength (MPa)	Young's modulus (GPa)	CTE (10^{-6}/°C)
N51A glass	–	2.2	64	72	7
Mullite	1850	3.17	128–185	181	4–5
Corning 7052	–	2.27	–	56.5	5.31

Table 3. Surface roughness of the fibers.

	PRD 166	Nextel 610	Saphikon
R_a (nm)	31.82	3.10	0.74
R_{max} (nm)	233.27	15.09	4.78
R_z (nm)	109.68	6.78	2.60

Table 4. Effects of thermal mismatch and surface roughness on the radial strain at the interface.

	PRD–166	Nextel 610	Saphikon
r, μm	10	5.5	40
α, $10^{-6}K^{-1}$	9	9	7.94 (⊥ to C–axis)
Radial compressive strain (due to roughness):			
R_a/r	0.003	0.0006	0.00002
R_{max}/r	0.027	0.0027	0.00012
R_z/r	0.011	0.0012	0.00007
Radial tensile strain (due to thermal mismatch):			
$\Delta\alpha \bullet \Delta T$ ($\alpha_{SnO_2}=5.23\times10^{-6}K^{-1}$, $\Delta T = 500K$)	0.002	0.0019	0.00136
Net radial strain (+: Tensile strain –: Compressive strain)	–0.025	–0.0008	+0.00123